Ultrafast reciprocal space investigation of cavity–waveguide coupling

M. Burresi,[1,2,*] D. van Oosten,[1,3] B. S. Song,[4,5] S. Noda,[4] and L. Kuipers[1]

[1]*Center for Nanophotonics, FOM Institute for Atomic and Molecular Physics (AMOLF),*
Science Park 104, 1098 XG Amsterdam, The Netherlands

[2]*European Laboratory for Non-linear Spectroscopy (LENS) and CNR-INO, Via N. Carrara 1, 50019 Sesto Fiorentino, Firenze, Italy*

[3]*Debye Institute for NanoMaterials Science, Utrecht University, P.O. Box 80000, 3508 TA Utrecht, The Netherlands*

[4]*Department of Electronic Science and Engineering, Kyoto University, Katsura, Nishikyo-ku, Kyoto 615-8510, Japan*

[5]*School of Information and Communication, Sungkyunkwan University, Janan-Gu, Suwon 440-746, Korea*

*Corresponding author: burresi@lens.unifi.it

Local information on the coupling mechanism between the photonic crystal nanocavity and the feeding waveguide is crucial to enable further improvements of the performance of these systems. Although several investigations on such a coupling have already been performed, information on the local dynamic properties remains hidden. Here, we present a reciprocal space investigation of the dynamics of light side-coupled to a photonic crystal nanocavity. We find that the coupling is promoted by Bloch harmonics having greater transverse momentum.   © 2011 Optical Society of America

    OCIS codes: 230.5298, 180.4243.

Photonic crystal nanocavities with a high quality factor and small modal volume [1–3] have been envisioned and realized for different types of applications. The most widespread strategies employed to feed nanocavities with light are based on the use of (i) in-line coupling [2] and (ii) side-coupling [1,3] between cavities and waveguides, as these allow a high degree of integration and tunability of their optical properties [4,5]. So far, this important coupling mechanism has been studied in the time and frequency domains with far-field experiments [4–6]. Qualitative considerations on the results shown in [6] suggested that such a coupling is promoted by large transverse momentum but a local insight on its dynamic nature has up to now not been given.

In this Letter, we present a phase-sensitive time-resolved near-field investigation of the loading and decay of light in a side-coupled photonic crystal nanocavity. After providing a direct visualization of the light as it couples to the cavity, a detailed analysis in reciprocal space lays bare the coupling mechanism between the side-coupled nanocavity and the adjacent waveguide.

The sample under investigation is shown in the inset in Fig. 1(a). The waveguide is formed by a single missing row of holes in a photonic crystal, whereas the cavity, with a resonant wavelength of 1534.6 nm, is formed by removing three holes. The interferometric optical setup is schematically depicted in Fig. 1(a) and thoroughly described in [7]. A near-field probe with a 200 nm thick aluminum coating and an aperture with a diameter of 200 nm is used to locally pick up the light propagating through the structure. By raster scanning the probe above the cavity–waveguide system, we are able to reconstruct the electric field distribution of light with phase sensitivity and subwavelength resolution. Moreover, we are able to perform time-resolved measurements. Here we use a picosecond-pulsed laser at a wavelength of 1534 nm with spectral width of 2 nm to probe the cavity–waveguide system. It is known that a near-field probe in the proximity of the nanocavity induces a frequency

shift of the cavity resonance [8]. From previous work on similar nanocavities and near-field probes [9], we know that the frequency shift induced by a coated near-field probe is of the order of $|\Delta\lambda| \approx 0.3$ nm. Because the spectral width of the pulse is much broader than the induced resonance shift, both the unperturbed and the probe-induced resonance of the cavity can be excited.

Figure 1(b) shows the amplitude detected in the near field at $t = 0$ ps, before the pulse enters the scanned area. As the delay time is increased by increasing the length of
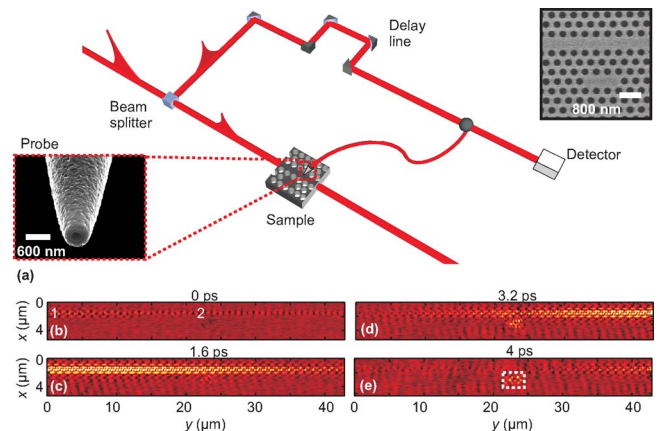
Fig. 1.   (a) Schematic representation of the setup. Linearly polarized light is coupled to the sample. Right-side inset: scanning electron micrograph of the investigated sample. The photonic crystal nanocavity is visible below the photonic crystal waveguide. Left-side inset: scanning electron micrograph of the near-field probe. The aluminum coating has a thickness of 200 nm and an aperture of 200 nm. (b)–(e) Normalized detected amplitude of the picosecond pulse propagating through the sample for different times. The color scale varies from 0 to 0.6 times the maximum value of the amplitude, in order to enhance the visibility of the signal obtained above the cavity. The consecutive images show a light pulse entering the access waveguide, loading the nanocavity [dashed box in (e)], and exiting from the waveguide.
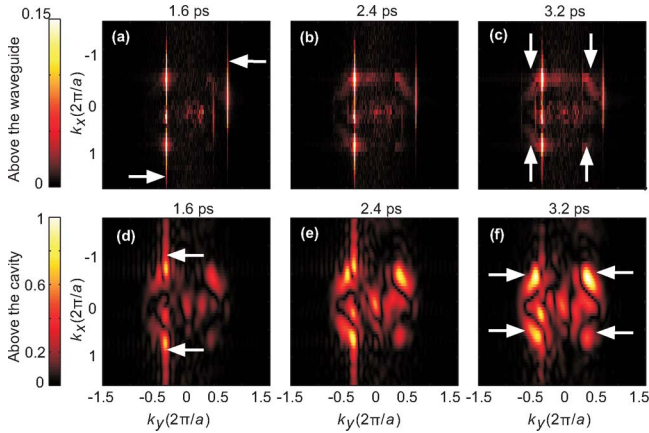
Fig. 2. (a)–(c) Normalized amplitude of the Fourier transform of the detected signal of the picosecond pulse propagating through the sample for different times. The bright features relate to the excited eigenstates. The subsequent images show the time evolution of the eigenstates. The white arrows in (a) indicate the fundamental (right arrow) and the −1 (left arrow) Bloch harmonics of the access waveguide. The white arrows in (c) indicate the four features that relate with the eigenstate of the cavity. The color scale varies from 0 to 0.15 in order to enhance the visibility of the eigenstate of the cavity. (d)–(f) Normalized amplitude of the Fourier transform of the signal detected above the area indicated by the dashed box in 1(e), for the same time delay as (a)–(c). The white arrows of (d) indicate the −1 Bloch harmonic of the access waveguide that spatially overlaps the cavity. The white arrows of (f) indicate the four features that relate with the eigenstate of the cavity. The color scale is normalized to the maximum of (f).

the reference branch, the time evolution of the light field is obtained [10]. In the consecutive measurements shown in Figs. 1(b)–1(e), we observe the pulse propagating through the access waveguide and coupling to the cavity (dashed box in Fig. 1(e)]. Figures 1(b)–1(e) show in both space and time the confinement of light in a photonic crystal nanocavity.

Whereas the basic dynamics of the mode coupling between the waveguide and the nanocavity is visible in Figs. 1(b)–1(e), detailed information about the mechanism of the coupling of the waveguide mode to the eigenstate of the nanoresonator is not revealed. Greater insight can be achieved by studying the dynamics of the eigenstates of the coupled system in reciprocal space. Exploiting the phase sensitivity of our measurements, we are able to unravel the mechanism of the mode coupling between cavity and waveguide via Fourier analysis [10]. Figure 2(a) shows the spatial frequencies of the optical field in Fig. 1(c) obtained by applying a Fourier transform to the complex-valued experimental data. With this procedure we can observe and separate the Bloch harmonics that compose the pulse traveling in the photonic crystal structure. The white arrows in Fig. 2(a) indicate the maxima that relate with the fundamental Bloch harmonic (the order of this Bloch harmonic is $n = 0$ [11]) and the −1 Bloch harmonic ($n = −1$) of the excited photonic eigenstate in the waveguide. Figures 2(b) and 2(c) show the spatial frequency distribution of the excited eigenstates at 2.4 and 3.2 ps, respectively. In particular, Fig. 2(c) shows that four new features arise as time

progresses. These four features, indicated by white arrows, correspond to the eigenstate of the nanocavity.

We perform a Fourier analysis of the signal detected directly above the cavity [dashed box in Fig. 1(e)] to have better insight into the coupling mechanism between waveguide and nanocavity. Figures 2(d)–2(f) show the amplitude of the Fourier transform for the same time delay as Figs. 2(a)–2(c). We find an excellent agreement between Fig. 2(f) and the corresponding calculated spatial frequencies for a photonic crystal nanocavity [1]. The two brighter features in Fig. 2(f) (white arrows) represent the −1 Bloch harmonic of the waveguide, which is also present in the scanned area above the nanocavity. As time progresses, the −1 Bloch harmonic peaks disappear, and the cavity eigenstate peaks increase in magnitude (white arrows in Fig. 2(f)]. Remarkably, these observations directly show that the −1 Bloch harmonic with its negative wave vector [Fig. 2(e)] is actually responsible for the light coupling to the nanoresonantor, as was previously argued by Smith et al. [6]. In their work they found that the mode of a side-coupled cavity couples to those modes in the waveguide having greater transverse momentum. Here, we are able to show that this coupling occurs through *only one* of the harmonics forming the waveguide Bloch mode. This happens because, on one hand, the −1 Bloch harmonic satisfies the k-matching condition necessary to excite the cavity eigenstate [Fig. 2(e) shows a clear overlap in the reciprocal space of the two modes] and, on the other hand, the spatial distribution of the −1 Bloch harmonic overlaps with the cavity mode. In fact, as has already been proven experimentally [12], the −1 Bloch harmonic is primarily located on the sides of the waveguide, and therefore it spatially overlaps with the cavity mode, whereas the fundamental Bloch harmonic is located in the center of the waveguide. Hence, the −1 Bloch harmonic, rather than the fundamental Bloch harmonic, is the promoter of the coupling between the nanocavity and the waveguide.

In order to directly investigate the extent to which the dynamics of the system can be controlled through the probe–cavity interaction, we analyze the time evolution of the amplitude $A_k^{cav}(t)$ of the cavity eigenstate. We
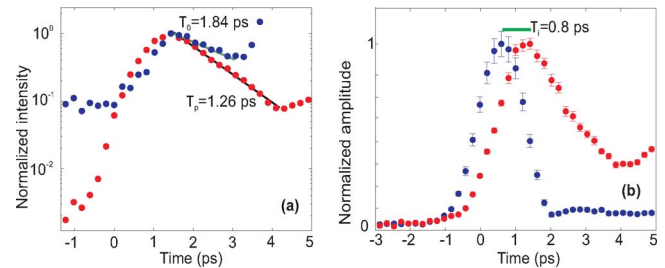
Fig. 3. (a) The red and blue dots relate to the time-dependent intensity (in logarithmic scale) of the eigenstate of the cavity and the eigenstate of the backward propagating light at position 1 of Fig. 1(b), respectively. The straight lines are the fits to the exponential decays. The rising of the signal at the end of both graphs (with blue higher than red) is caused by the backward propagating pulse reflected at the end facet of the waveguide. The x axis of the blue-dotted graph has been shifted in order to better compare the two graphs. (b) Time-dependent amplitude detected at position 2 of Fig. 1(b) (blue dots, with lower end dot) and of the eigenstate of the nanocavity (red dots).

consider the time-dependent intensity $I_k^{cav}(t) = [A_k^{cav}(t)]^2$, shown in Fig. 3(a) (red dots), as the time duration of $I_k^{cav}(t)$ directly relates to the photon lifetime of the cavity. Initially the cavity is loaded by the pulse, and the energy flow from the waveguide to the cavity exceeds the reverse flow [left half of Fig. 3(a)]. Thereafter, the predominant flow of energy is from the cavity to the waveguide, and the signal exponentially decreases. This process is clearly shown in Fig. 3(b), which compares the amplitude $A_k^{cav}(t)$ (red dots) with the amplitude of the pulse propagating in the waveguide detected at position 2 in Fig. 1(b) (blue dots). The two envelopes show a clear delay between the two maxima and a different slope of the rising edge. This is given by the interplay between the loading of the cavity by the pulse and the simultaneous leaking of the cavity itself. The delay time between the two maxima can be considered the loading time $\tau_i \approx 0.8$ ps of the cavity.

From the exponential decay time of $I_k^{cav}(t)$ in Fig. 3(a) (black line), we determine that the photon lifetime in presence of the probe–zcavity interaction is $\tau_p = 1.26$ ps. As can be seen in Fig. 3(b), the loading time τ_i is shorter then the lifetime, because the loading is cut short by the finite duration of the pulse. In order to compare τ_p with the unperturbed photon lifetime τ_0, we studied the pulse duration of the light exiting the cavity and propagating backward in the waveguide. By performing a Fourier analysis of the area above position 1 in Fig. 1(b), we study the time evolution of the amplitude $A_k^{w.g.}(t)$ of the Fourier components corresponding to the backward propagating pulse. $I_k^{w.g}(t) = [A_k^{w.g}(t)]^2$, plotted in Fig. 3(a) as blue dots, shows a clear exponential tail. From the fit we obtained the unperturbed $\tau_0 \approx 1.84$ ps. Hence, the presence of the probe above the cavity induces an average (averaged over different probe positions above the nanocavity) change of the photon lifetime of $\Delta\tau_0 = (\tau_1 - \tau_0)/\tau_0 \approx -0.3$.

We showed a reciprocal space ultrafast near-field investigation of light coupling to a side-coupled photonic crystal nanocavity. Exploiting the phase sensitivity of our measurements, we showed that the coupling between the eigenstate of the waveguide and the eigenstate the nanoresonator is actually promoted by the waveguide

−1 Bloch harmonic, because it satisfies the coupling conditions in both real and reciprocal space. We furthermore succeeded in measuring the lifetime of the cavity and the degree of perturbation of the near-field probe on such a lifetime measurement, observing the dynamics of the eigenstate of the waveguide and cavity, respectively.

References

1. Y. Akahane, T. Asano, B. S. Song, and S. Noda, Nature **425**, 944 (2003).
2. T. Tanabe, M. Notomi, S. Mitsugi, A. Shinya, and E. Kuramochi, Appl. Phys. Lett. **87**, 151112 (2005).
3. T. Uesugi, B.-S. Song, T. Asano, and S. Noda, Opt. Express **14**, 377 (2006).
4. S. M. Spillane, T. J. Kippenberg, O. J. Painter, and K. J. Vahala, Phys. Rev. Lett. **91**, 043902 (2003).
5. T. Yoshinori, J. Upham, T. Nagashima, T. Sugiya, T. Asano, and S. Noda, Nat. Mater. **6**, 862 (2007).
6. C. J. M. Smith, R. M. D. L. Rue, M. Rattier, S. Olivier, H. Benisty, C. Weisbuch, T. F. Krauss, R. Houdre, and U. Oesterle, Appl. Phys. Lett. **78**, 1487 (2001).
7. M. Sandtke, R. J. P. Engelen, H. Schoenmaker, I. Attema, H. Dekker, I. Cerjak, J. P. Korterik, F. B. Segerink, and L. Kuipers, Rev. Sci. Instrum. **79**, 013704 (2008).
8. A. F. Koenderink, M. Kafesaki, B. C. Buchler, and V. Sandoghdar, Phys. Rev. Lett. **95**, 153904 (2005).
9. M. Burresi, T. Kampfrath, D. van Oosten, J. C. Prangsma, B. S. Song, S. Noda, and L. Kuipers, Phys. Rev. Lett. **105**, 123901 (2010).
10. R. J. P. Engelen, Y. Sugimoto, H. Gersen, N. Ikeda, K. Asakawa, and L. Kuipers, Nat. Phys. **3**, 401 (2007).
11. N. W. Ashcroft and N. D. Mermin, *Solid State Physics* (Brooks Cole, 1976).
12. M. Sandtke and L. Kuipers, Phys. Rev. B **77**, 235439 (2008).